Geological Survey
of Canada

Current Research
2001-D21

Clay mineralogical study of indurated seafloor sediment samples from the Lihir area, Papua New Guinea

B. Obina, J.B. Percival, and P.A. Hunt

2001

Natural Resources Canada Ressources naturelles Canada

Canada

©Her Majesty the Queen in Right of Canada, 2001
Catalogue No. M44-2001/D21E
ISBN 0-660-18445-1

Available in Canada from the
Geological Survey of Canada Bookstore website at:
http://www.nrcan.gc.ca/gsc/bookstore (Toll-free: 1-888-252-4301)

A copy of this publication is also available for reference by depository libraries across Canada through access to the Depository Services Program's website at http://dsp-psd.pwgsc.gc.ca

Price subject to change without notice

All requests for permission to reproduce this work, in whole or in part, for purposes of commercial use, resale or redistribution shall be addressed to: Geoscience Information Division, Room 200, 601 Booth Street, Ottawa, Ontario K1A 0E8.

Authors' addresses

B. Obina *(bobina@yahoo.com)*
2-93 Flora Street
Ottawa, Ontario K2P 1A7

J.B. Percival *(jpercival@nrcan.gc.ca)*
P.A. Hunt *(phunt@nrcan.gc.ca)*
Mineral Resources Division, Ottawa
Geological Survey of Canada
601 Booth Street
Ottawa, Ontario K1A 0E8

101-03600/

Clay mineralogical study of indurated seafloor sediment samples from the Lihir area, Papua New Guinea

B. Obina, J.B. Percival, and P.A. Hunt
Mineral Resources Division, Ottawa

Obina, B., Percival, J.B., and Hunt, P.A., 2001: Clay mineralogical study of indurated seafloor sediment samples from the Lihir area, Papua New Guinea; Geological Survey of Canada, Current Research 2001-D21, 9 p.

Abstract: Detailed studies of samples collected from two seafloor cruises to the Lihir area in Papua New Guinea continue. In 1994, a detailed study of the Tabar–Lihir–Tanga–Feni island chain in the New Ireland fore-arc basin was conducted aboard the R/V *Sonne* (cruise SO-94). The discovery of four new seamounts led to further investigations in 1998 (cruise SO-133). Edison Seamount was determined to be hydrothermally active and marked a new type of setting on the seafloor for shallow-marine hot springs. Conical Seamount, a dormant cone, is characterized by distinctive epithermal-style gold mineralization.

Two unusual indurated sediment samples from Conical Seamount were the focus of this study. They are composed of amorphous silica/glass and/or iron oxide layers (crusts), iron-bearing smectite and calcite. These minerals occur in a low-temperature hydrothermal environment, indicating that these samples are the end product of submarine hydrothermal alteration and sea-water/rock interactions.

Résumé : Des études approfondies d'échantillons prélevés lors de deux expéditions ayant pour but d'étudier le fond marin de la région de Lihir, en Papouasie–Nouvelle-Guinée, se poursuivent. En 1994, une étude approfondie dans l'arc insulaire qui comprend les îles Tabar, Lihir, Tanga et Feni, dans le bassin d'avant-arc de New Ireland, a été effectuée à bord du navire R/V *Sonne* (expédition SO-94). La découverte de quatre nouveaux monts sous-marins a donné lieu à d'autres travaux en 1998 (expédition SO-133). Le mont sous-marin Edison serait hydrothermiquement actif et représenterait un nouveau type d'environnement sur le fond marin pour les sources chaudes en eaux peu profondes. Le mont sous-marin Conical, un cône inactif, est caractérisé par une minéralisation d'or de type épithermal.

La présente étude a porté sur deux échantillons exceptionnels de sédiments consolidés provenant du mont sous-marin Conical. Ces sédiments sont composés de silice/verre amorphe et/ou de couches d'oxyde de fer (croûtes), de smectite ferrifère et de calcite. Ces minéraux se rencontrent dans un environnement hydrothermal de basse température, ce qui indique que les échantillons sont le produit final de l'altération hydrothermale sous-marine et d'interactions entre l'eau de mer et les roches.

INTRODUCTION

As part of the continuing studies of seafloor samples collected during the 1998 EDISON (Epithermal Deposits Southwestern Pacific Ocean) cruise (SO-133), two samples were selected for detailed work. The sediment samples retrieved from the Lihir Island area (Fig. 1), in particular from the vicinity of Conical Seamount (Fig. 2), appeared weakly indurated and consisted of several layers of oxide crusts interlayered with foraminiferal ooze. Shipboard X-ray analyses indicated the presence of smectite and sulphides (Percival, 1998), indicative of a hydrothermal environment. Evidence from the 1994 and 1998 cruises have shown that hydrothermal activity is occurring in this rifted fore-arc setting, with attendant epithermal-style gold mineralization (Herzig and Hannington, 1995, 1998).

This report summarizes the petrographic and mineralogical characteristics of samples 74 GTVA and 83 GTVA, with insight into the origin of the clay and associated minerals, and nature of induration. This study formed the basis of a B.Sc. thesis at Carleton University, Ottawa, Ontario (Obina, 2000).

GEOLOGICAL SETTING

Lihir Island is part of the Tabar–Feni island chain in the Bismarck Archipelago. The Archipelago is located in the fore-arc basin parallel to the Manus–Kilinailau subduction zone northeast of Papua New Guinea (Fig. 1). Detailed mapping and extensive sampling were completed during two cruises aboard the German research vessel, R/V *Sonne*, in 1994 and 1998 (Herzig and Hannington, 1994, 1998).

Four seamounts were discovered in 1994 near Lihir Island, and were named Edison, TUBAF (named for Technische Universität Bergakademie Freiberg), Conical, and New World (Fig. 2). Methane anomalies and faunal communities (ie. clam beds and barnacles) associated with hydrothermal vents were observed by TV grab at Edison in 1994. Conical Seamount, the largest of the four discovered in 1994, is 2.5 km in diameter at the base, and rises more than 600 m above the seafloor to a conical peak with a narrow, flat, fissured summit at a depth of 1050 m. It lies 10 km south of Lihir and about 25 km south of the Ladolam gold deposit. At Conical Seamount, epithermal-style gold mineralization was confirmed (Herzig and Hannington, 1998). Discovery of more

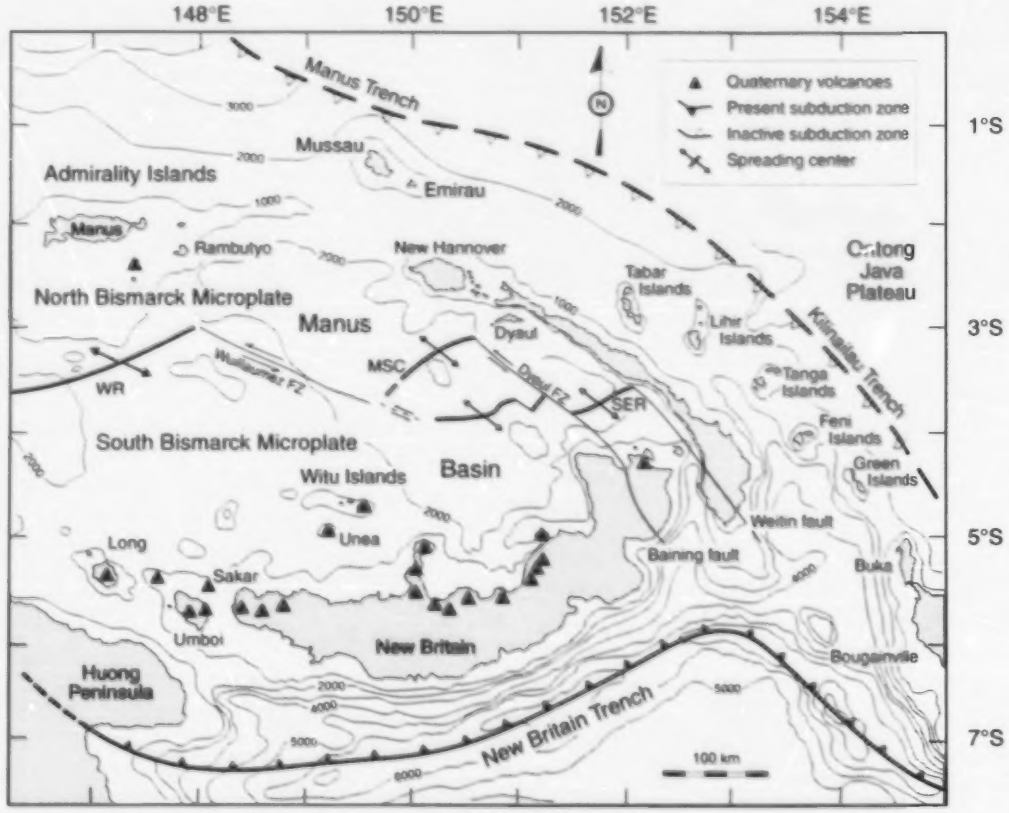

Explanation: MSC = Manus Spreading Center; SER = Southeastern Rift; WR = Western Ridge

Figure 1. *Regional map of the Tabar–Lihir–Tanga–Feni island chain* (after *Herzig and Hannington, 1998*).

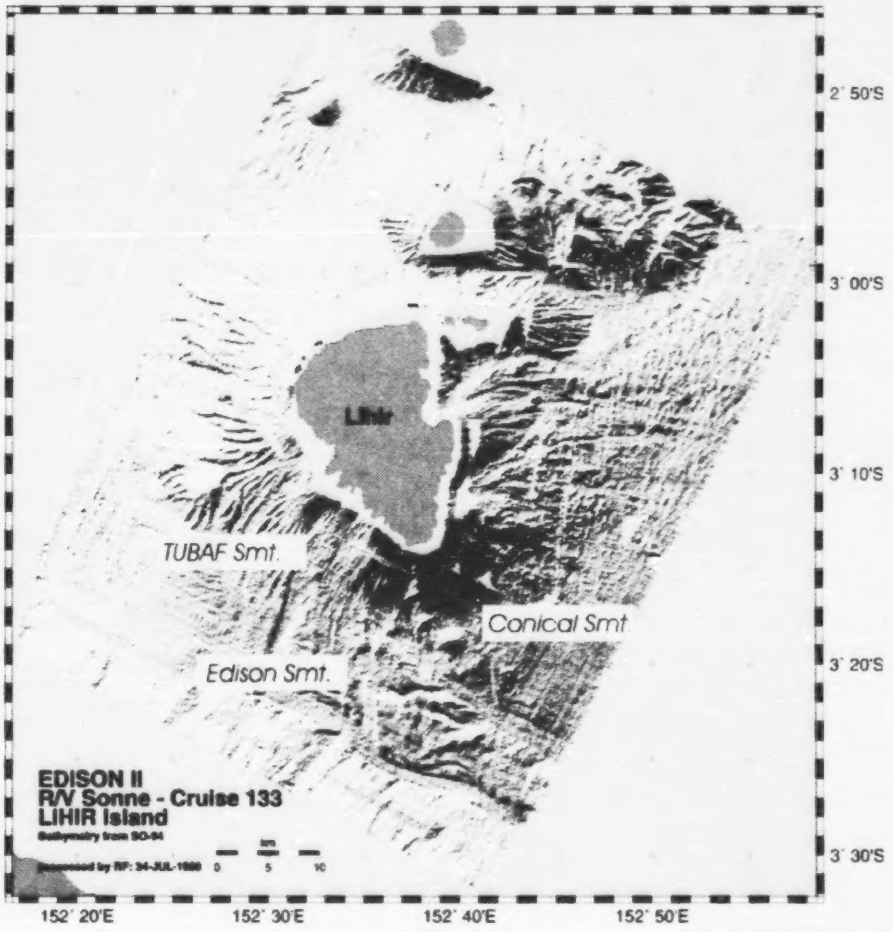

Figure 2.

Detailed multibeam bathymetric map of Lihir Island group and location of seamounts (after *Herzig and Hannington, 1998*).

young volcanic cones in the area south of Lihir Island during 1998 demonstrates that volcanism in the New Ireland Basin is now focused in the active tectonic zone of the Lihir Group.

SAMPLING AND METHODS

Sample 74 GTVA was collected on July 30, 1998, from a small seamount northwest of Conical Seamount at a depth of 1489 m. A TV-grab (a TV-guided dredge) around the edge of the cone and down the flanks recovered about 200 kg of mostly indurated and veined carbonated sands. This area is mostly covered with pelagic sediment, but also has coarser, up to pebble-sized, material. Sample 74 GTVA comprises a variegated and extensively veined, indurated sediment, although most of it is soft enough to break by hand. Anastomosing veins of red, green, and black material are common.

Sample 83 GTVA was collected on July 31, 1998, from the top of Conical Seamount at a depth of 1091 m. The TV-grab recovered 75 kg of boulder- and cobble-sized, highly altered lava samples. The grab contained samples of homogenous grey, zonally altered ankaramite, some with thick oxide crusts. Franklin et al. (1998) reported that the larger samples demonstrated that zonal alteration proceeded along propagating fractures to develop distinct zones of clay-rich, silica-rich, and sulphidized ankaramite. The rock disintegrated into cobble-sized fragments on sampling, breaking along intensely altered fractures. All samples contained disseminated pyrite.

Sample preparation for mineralogical analysis was difficult due to extreme fragility of the samples upon drying. Samples were prepared for thin sectioning by impregnation with Petropoxy 154® to strengthen the sediment.

X-ray diffraction (XRD) analyses involved the separation of bulk samples into a series of ten subsamples by scraping with a spatula. Sample 74 GTVA was subdivided into yellow, green, white, orange, and red sub-samples. Sample 83 GTVA was subdivided into brown, red, yellow, white, and grey scrapings. Using an agate mortar and pestle, each of the scrapings was gently ground in distilled water. Smear mounts were prepared by pipetting a suspension onto glass slides that were air-dried overnight. The smears were then analyzed by powder X-ray diffractometry (XRD) from 2° to 70° 2θ to determine qualitative mineralogy. A Philips PW1710 automated powder diffractometer, equipped with a graphite

monochromator, Co Kα radiation set at 40 kV and 30 mA was used. Samples were then reanalyzed after being glycol-saturated and heat-treated (two hours at 550°C) to identify the different clay mineral species.

Ten grain mounts were made for examination under a scanning electron microscope (SEM). All grain mounts were prepared by pipetting a very dilute (<10–20 ppm) suspension onto carbon-impregnated tape. Two thin sections from groups 74 GTVA and 83 GTVA were also selected for detailed analyses. All samples were carbon-coated before examination using a Leica Cambridge Stereoscan S360 scanning electron microscope (SEM). The SEM was equipped with an Oxford/Link eXL-II energy-dispersion X-ray analyzer, Oxford/Link Pentafet Be window/light element detector, and an Oxford/Link Tetra backscattered electron detector. The SEM is operated at an accelerating voltage of 20 kV. The SEM images were captured at 768 x 576 x 256 greyscale and digitally stored for further processing.

Six thin sections taken from sample 74 GTVA and 83 GTVA were coated with 250 Å of carbon and analyzed for major and trace elements with a Cameca Camebax MBX electron microprobe.

RESULTS

Petrographic analyses

In hand specimen, 74 GTVA-2B shows interveined features forming a braid-like pattern (Fig. 3a). Prominent red, and yellow-green layers of sediment are visible. Within the white and yellow-green layers, there are 125 µm-sized aggregates of circular, calcareous material; however, the overall particle size is less than 4 µm (silt to clay). Sample 83 GTVA-3A does not show any interveining features nor layering, but there are variegated patches of orange-red, yellow-green, grey-white, and black (Fig. 3b). This sample is calcareous with visible grains of disseminated pyrite. Particle size is similar to sample 74 GTVA-2B (silt to clay, < 4 µm).

Figure 3a. *Scanned image of thin section 74 GTVA. Marked circles indicate areas of study for the SEM and electron microprobe.*

Figure 3b. *Scanned image of thin section 83 GTVA. Marked circles indicate areas of study for the SEM and electron microprobe.*

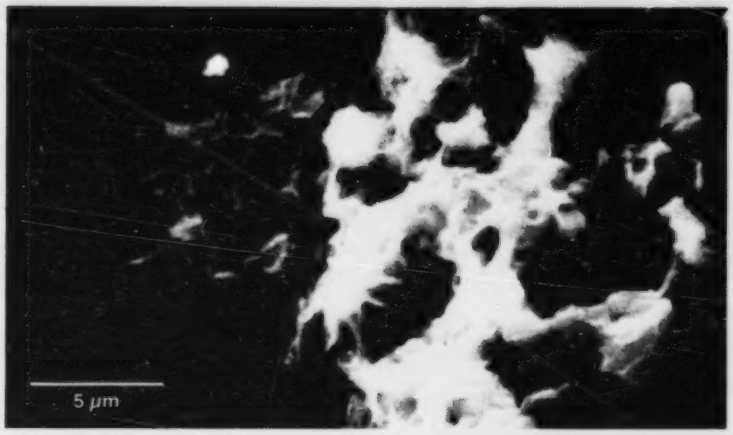

Figure 4.

Scanning electron photomicrograph of a cluster of smectite grains showing typical crenulated, wispy texture (backscattered electron image, BSI).

Figure 5.

Scanning electron photomicrograph of a plagioclase feldspar crystal imbedded in amorphous silica/glass (image taken from the green layer in sample 74 GTVA; BSI).

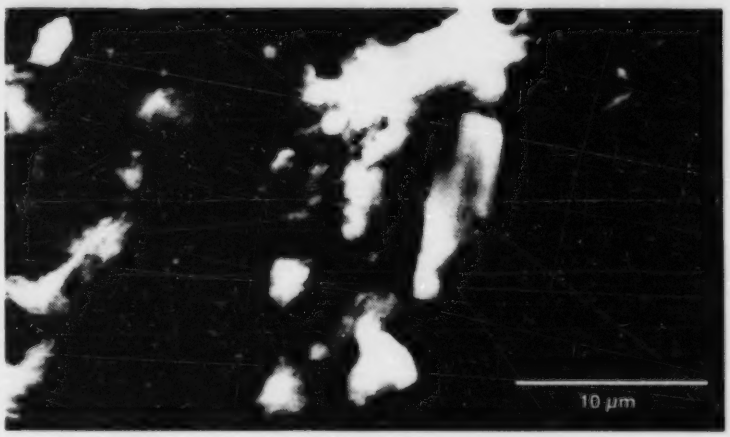

Sample 74 GTVA-2A consists of layers of red 'crusts' and yellow-green sediments. On average, the red layers comprise 35 to 60% of the sample. The red layers range in thickness from 0.4 to 11.6 mm and appear to be massive in texture. The yellow-green layers range from 3.1 to 11.4 mm thick, and are fine grained, with foraminifers constituting up to 80% of the layers. Angular to elongate fragments of plagioclase, and subangular discrete grains of pyroxene and calcite, were also observed in the yellow-green layer. In total, these minerals make up from 5 to 10% of the sample. Throughout the red layers, fractures are prominent. Compositionally, sample 74 GTVA-2A is a foraminiferal ooze with varicoloured 'crusts' or 'veins'.

In comparison, sample 83 GTVA-3A contains more mineral fragments and fewer foraminifers. The subangular to angular fragments include pyroxene, plagioclase, and biotite set within the foraminifer-rich matrix which constitutes 90% of the sample.

X-ray diffraction analyses

Results of XRD analyses of the various coloured layers in sample 74-GTVA show that smectite and calcite are the dominant minerals. All subsamples contain X-ray amorphous components (silica/glass and/or Fe-oxide) which yield poor-quality X-ray patterns. The white subsample also contains minor to trace amounts of aragonite and possibly kutnohorite ($CaMn(CO_3)_2$) with an X-ray peak at 3.0Å. Sample 83 GTVA-3A also contains abundant calcite and smectite and an X-ray amorphous component. Minor to trace amounts of plagioclase feldspar, illite/mica, quartz, and chlorite (and/or kaolinite) were detectable in the yellow subsample. Minor to trace minerals in the grey subsample include chlorite or kaolinite (note that X-ray peaks are too low intensity to distinguish between these two minerals). The brown subsample was completely X-ray amorphous.

Scanning electron microscope analyses

In SEM analyses, it was possible to observe the texture of each sample and identify the individual grains and minerals present through EDS (energy dispersive X-ray spectrometer) analyses. Figure 4 illustrates the common crenulated, wispy texture of smectite grains observed in the yellow subsample of 74 GTVA-2B. This was also observed in the yellow subsample of 83 GTVA-3A. The green subsample of 74 GTVA-2B displays a globular, clumpy texture and is probably a glass or mixture of amorphous silica and Fe-oxides (Fig. 5). Detailed examination of the grain mounts of each of

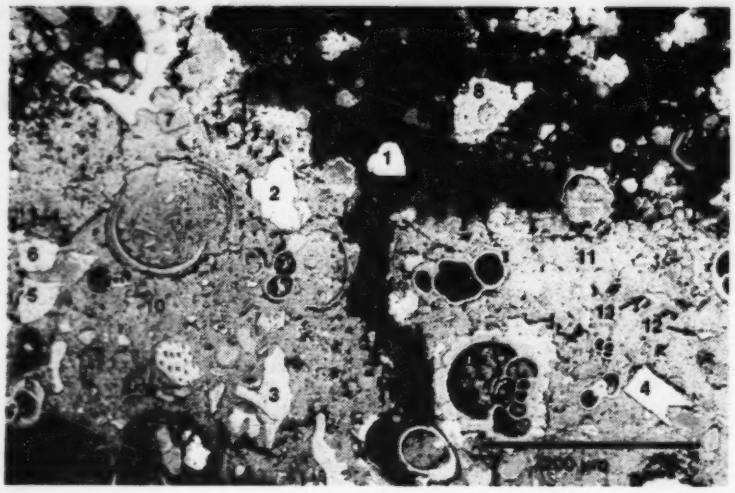

Figure 6.

Scanning electron photomicrograph of 74 GTVA-2A matrix. (1) Fe-bearing titanite, (2, 4) pyroxene, (3) calcareous fragment, (5, 6, 8) shell fragment, (7) plagioclase feldspar, (9) amorphous silica/glass, (10–13) silica-calcite ooze (BSI).

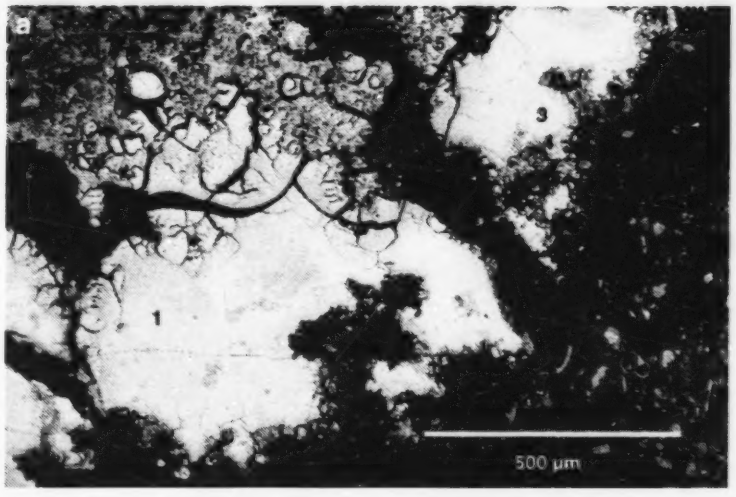

Figure 7a.

SEM photomicrograph showing the massive texture of the red and orange layers/crusts in sample 74 GTVA. Note EDS analyses for spots 1 to 5 consists of Si, Fe, P and Ca; spot 6 consists of Si, Fe, P, Ca with minor K, Mg, and Na (BSI).

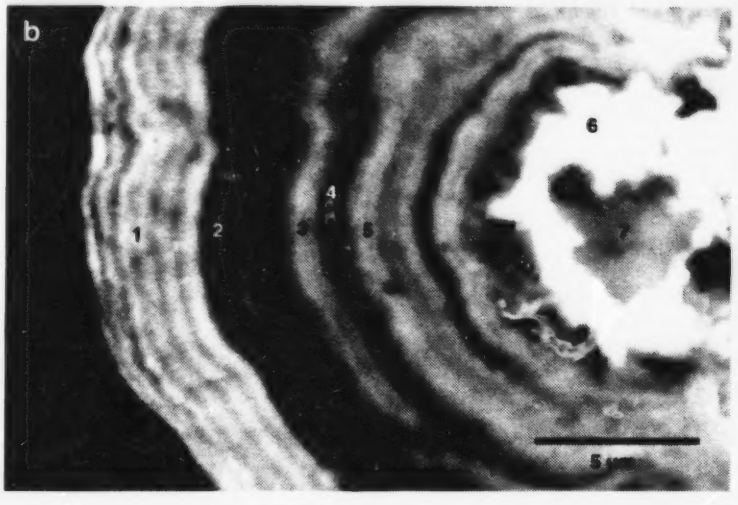

Figure 7b.

SEM photomicrograph of a Mn-oxide nodule (a close-up of the concentric banding in 74 GTVA). (1) Mn, O, Mg, Ca, and K, (2) Mn and O, (3) Mn, O, Mg, and Ca, (4) Mn and O, (5) Mn, O, and Ca, (6) Mn, O, and major Mg, and (7) Mn, O, and minor Mg (BSI).

the coloured layers enabled a qualitative differentiation amongst them mineralogically, the results of which are supported by the XRD data.

In sample 74 GTVA-2B, Fe-oxide-coated glass/amorphous silica dominates the yellow subsample. It is interpreted to be volcanic glass because of its composition shown by EDS spectra (major Si, Fe, O, and minor K, Ca, Mg, Al, and Na). Traces of plagioclase, pyroxene, and possibly apatite are also present. Iron-bearing smectite was observed along with Fe-titanite and plagioclase in the green subsample. The white subsample is dominated by smectite and calcite. The orange and red subsamples contain grains with the composition of Fe, Si, O, P, and Ca. A minuscule grain from the red layer was extracted from sample 74 GTVA for X-ray analysis (using a Debye-Sherrer Camera). Results indicated it was X-ray amorphous.

The brown and red subsamples of 74 GTVA contain mostly iron-coated silica with phosphorus, however, Mn-oxide nodules are seen in the brown subsample and not in the red. Smectite, ilmenite, calcite, and titanomagnetite are common in the yellow sample. Both the white and grey subsample have grains with similar composition to the amorphous silica/glass. However, some grains contain Mg in addition to the Al, Si, Ca, Fe, and O, suggesting smectite. There were also high concentrations of Mn in the white and grey subsamples, suggesting the presence of Mn-oxide nodules.

The SEM analyses of thin sections 74 GTVA-2A (Fig. 3a) and 83 GTVA-3A (Fig. 3b) enabled an overview of the textures and nature of the minerals. The greenish layers in 74 GTVA-2A, which represents the pelagic sediment, contain a heterogenous mixture of pyroclastic (glass) fragments. The sample is composed of a matrix rich in foraminifers and angular grains of plagioclase (some are elongate), pyroxene, Fe-titanite, silica-calcite ooze, and calcareous fragments (Fig. 6). Clay minerals (e.g. smectite) were difficult to distinguish due to the fine-grained nature, the overwhelming presence of calcite, and coating by amorphous Fe-oxides. The red and orange layers in sample 74 GTVA-2A have a massive texture (Fig. 7a). Towards the outer edges, the sediment is desiccated and cracked. A detailed examination of the outer edges illustrates a colloform, concentric banding made up of Mn-oxides with traces of Mg, Ca, K, and O. The EDS analyses along a transect from the outer edge of the nodule towards the centre show a decrease in Mg content; however, the Mn content was consistent (Fig. 7b). Observed within this sample were calcareous shells/foraminifers infilled with angular grains of amorphous silica/glass, calcite, plagioclase, and pyroxene.

Sample 83 GTVA-3A appears to contain more pyroclastic fragments than sample 74-GTVA-2A (titanomagnetite, plagioclase, quartz, and Fe-oxides) with the matrix being silica-calcium carbonate ooze. The ratio of matrix to fragments is 30 to 70% for sample 83 GTVA-3A, and 40 to 60% for sample 74 GTVA-2A.

Table 1. Comparison of analyses of some iron-bearing dioctahedral nontronites as cited in Weaver and Pollard (1973) with microprobe analyses from samples 74 GTVA and 83 GTVA.

Sample	1	2	3	4	5	6
SiO_2	56.91	39.52	43.05	51.39	53.5	53.28
Al_2O_3	22.65	18.48	6.40	4.01	4.32	5.54
Fe_2O_3	6.29	12.60	17.86			
FeO	0.11		0.10	31.04*	28.76*	30.3*
MgO	3.62	3.27	4.46	6.69	4.27	3.85
CaO	1.47	2.72	2.92	2.92	1.2	0.36
Na_2O	0.18	0.10		1.83	0.83	1.26
K_2O	0.74	0.50		1.32	4.92	4.71
TiO_2	0.65	1.88		0.04		0.04
H_2O^+	7.34	12.10	23.93			
H_2O^-		9.04	23.93			
Cr_2O_3			0.87			
MnO				0.18	0.02	0.06
BaO				0.03		
P_2O_5				0.24		
Cl				0.13	1.15	0.6
F				0.16		
Total	99.96	100.21	100.04	99.98	99.98	100

1. Altschuler et al. (1963): marine clay associated with Bone Valley phosphates, Fla., USA.
2. Alietti (1960): hydrothermal alteration of basaltic tuff.
3. Köster (1960): altered basalt.
4. 74 GTVA-2A-Grain #2
5. 83 GTVA-3A-Grain #6
6. 83 GTVA-3A-Grain #7

* = total Fe expressed as FeO

Electron microprobe analyses

Low weight per cent totals (e.g. ~70–90%) obtained by microprobe analyses are consistent with clay mineral analyses reflecting their fine-grained nature of the matrix and high porosity. Analyses of smectite grains from 74 GTVA and 83 GTVA are given in Table 1 in columns 4 to 6 in comparison to published data for nontronite. Data reveal that the SiO_2 and FeO contents are dominant in both samples. Sample 74 GTVA and 83 GTVA have a higher total Fe and lower Al_2O_3 content than columns 1 and 2. However, the Al_2O_3 content compares well with that of column 3. The high total FeO content may indicate the presence of free Fe-oxides coating the smectite. Inconsistencies in the CaO, Al_2O_3, TiO_2, MgO, K_2O, and P_2O_5 contents may reflect mixtures rather than specific minerals.

DISCUSSION

Velde (1985) considers two types of facies occurring under hydrothermal alteration conditions: a low-temperature nontronite-alkali zeolite facies and a higher temperature celadonite-Ca-zeolite-Al smectite-analcime facies. Nontronite is the major clay mineral formed as a replacement of volcanic phases. Its low Al/Fe ratio has been interpreted by Velde (1985) to indicate a hydrothermal origin. Murnane and Clague (1983) studied nontronite from a low-temperature hydrothermal system on the Juan de Fuca Ridge. They stated

that nontronite formed from newly established hydrothermal systems associated with the propagating rift segment. As a result, nontronite formed by the precipitation of Fe, Mg and Si when hydrothermal fluids mixed with subsurface seawater.

Microprobe data from this study were comparable to the published chemical analyses of nontronites from similar environments (Table 1). The variety of smectite from Conical Seamount may indeed be a nontronite, however, in order to confirm this, samples need to be pretreated to remove free Fe-oxides before XRD and SEM analyses.

XRD analyses for sample 74 GTVA-2B and 83 GTVA-3A showed calcite and smectite as the abundant minerals. Induration of these samples may be due to the presence of a calcareous and smectite cement; however, the distinction between these two minerals in the matrix was difficult under the SEM. Amorphous silica/glass and/or Fe-oxides, Fe-bearing smectites, as well as primary volcanic minerals such as pyroxene and plagioclase were observed under the SEM. The presence of smectite and amorphous silica/glass and/or Fe-oxides suggests a low-temperature environment and supports the idea that these samples are the end product of low-temperature submarine hydrothermal alteration and sea-water/rock interaction (Percival et al., 1999).

During the SO-133 cruise, Winn et al. (1998) investigated sediment samples collected by box and piston cores to reconstruct the recent volcanic history of the New Ireland fore-arc. They carried out their analyses by concentrating on ash layers within the sediment cores. At station 57-GKG, there were concretionary crusts that were lithified by calcareous cement forming 'hardgrounds'. These 'hardgrounds' are in close proximity to a horst-and-graben structure south of Lihir Island that was populated with clams in a gas-rich (methane) environment. Similar calcareous cementation may be present in the sediments at Conical and Edison. However, it will be essential to test whether they are cemented due to methanotrophic or sulphotrophic processes through stable isotopic analyses.

Samples 74 GTVA and 83 GTVA can be considered as weakly indurated sediments (at time of collection) with associated variegated layers or 'crusts'. These samples are proximal to zones of diffuse thermal fluids which have directly contributed to the precipitation of smectite, Mn- and Fe-oxides, and sulphides at the two seamounts. Fractures and varicoloured 'crusts' do occur in both samples and their presence indicates hydrothermal alteration.

During cruise SO-94, Edison Seamount was found to have diffuse venting at two sites characterized by live clam beds, shimmering water, sulphidic muds, and methane-plume anomalies in the water column. This appeared to be associated with black muds containing Mg-rich smectite, possibly saponite (Percival, 1994; Percival et al., 1999). Percival and Ames (1993) noted that Mg-rich (or Fe-rich) smectites are products of active vent sites on the seafloor as a result of the hydrolysis of hydrothermal fluids, their reaction with sediments and mixing with ingressing seawater. Although seafloor venting was not evident at Conical Seamount, alunite with Mg-smectite and base-metal sulphides (discovered during SO-94) were present, indicating circulation of warm, acidic hydrothermal fluids within the subsurface sediments (Percival et al., 1999). Thus, smectite and associated minerals found in variegated 'crusts' or layers and within the pelagic sediments of samples 74 GTVA and 83 GTVA indicate formation by precipitation from subsurface low-temperature fluids, likely the residual components of 'spent' higher temperature hydrothermal fluids.

SUMMARY

Herzig and Hannington (1995) reported that the Lihir Island area is the first documented evidence of modern seafloor hydrothermal activity in a rifted fore-arc setting. Samples collected during the EDISON (SO-133) cruise aboard the R/V *Sonne* provided an opportunity to study, in detail, indurated sediments of low-temperature hydrothermal origin from this unique setting. The objectives of this study were to characterize samples 74 GTVA and 83 GTVA, to ascertain why they are indurated, and to determine the origin of the clay minerals.

Samples 74 GTVA and 83 GTVA are variegated, weakly indurated sediments. They comprise a matrix rich in foraminifers and lava fragments (including glass, pyroxene, plagioclase, quartz, and Fe-oxides). Clay minerals in the matrix and in the 'crusts' or layers are dominated by smectite, minor to trace amounts of chlorite and illite/mica. Based on SEM and microprobe analyses, the smectite appears to be nontronitic. Absolute confirmation can only be accomplished by chemical pretreatment to remove free Fe-oxides before XRD analyses. Within the fine-grained matrix, an X-ray amorphous component occurs with a composition of major Si, Fe, O and minor K, Ca, Mg, Al, Na, and P. This was interpreted to be either Fe-coated amorphous silica or a volcanic glass.

Amorphous silica/glass and/or Fe-oxides and smectite indicate low-temperature hydrothermal fluid interaction with the pelagic sediments. Samples 74 GTVA and 83 GTVA are weakly indurated due to the presence of a calcareous-smectite cement formed by interaction with foraminiferal tests and low-temperature hydrothermal fluids percolating from within the seamounts.

ACKNOWLEDGMENTS

The authors are grateful to A. Roberts (GSC) who provided powder camera analyses; P. Jones (Carleton University) for electron microprobe analyses; T. MacDonald (Holy Trinity HS) for XRD assistance; and R. Lacroix (GSC) for assistance with SEM photomicrographs. Thanks to B. Cousens (Carleton University) for his time, advice and discussions, and to M.D. Hannington, I.R. Jonasson, and G.M. LeCheminant (all GSC) for critical review of this paper. Cruise SO-133 was made possible through the German Ministry of Education, Science, Research and Technology (BMBF) through Grant No. 03G0133A to Freiberg University of Mining and Technology.

REFERENCES

Alietti, A.
1960: Su di una nontronite poco ferrifera di Chiampo (Lesseni): Società Tipografica Editrice Modenese, v. 1960, p. 33–44 (in Italian).

Altschuler, Z.S., Dwornik, E.J., and Kramer, H.
1963: Transformation of montmorillonite to kaolinite during weathering: Science, v. 141, p. 148–152.

Franklin, J., Gemmell, B., Jonasson, I., Perfit, M., Franz, L., and Seifert, T.
1998: Sample descriptions of dredge and TV-grab sampling stations; *in* Volcanism, Hydrothermal Processes and Biological Communities at Shallow Submarine Volcanoes of the New Ireland Fore-Arc (Papua New Guinea), (eds.) P.M. Herzig, MD. Hannington, and Shipboard Scientific Party; Report of *Somne* SO-133, BMBF FK 03G0133A, Freiberg University of Mining and Technology, p. 34–82.

Herzig, P.M and Hannington, MD.
1994: Summary of results; *in* Tectonics, Petrology and Hydrothermal Processes in Areas of Alkaline Island-Arc Volcanoes in the Southwest Pacific: The Tabar–Lihir–Tanga–Feni Island Chain, Papua New Guinea, (eds.) P.M. Herzig, MD. Hannington and Shipboard Scientific Party; Report of *Somne* SO-94, BMFT FK 03G0094A0, Freiberg University of Mining and Technology, p. 6–16.
1995: Hydrothermal activity, vent fauna, and submarine gold mineralization at alkaline fore-arc seamounts near Lihir Island, Papua New Guinea; *in* Proceedings Pacific Rim Congress, Australian Institute of Mining and Metallurgy, p. 279–284.
1998: Summary of results; *in* Volcanism, Hydrothermal Processes and Biological Communities at Shallow Submarine Volcanoes of the New Ireland Fore-Arc (Papua New Guinea), (eds.) P.M. Herzig, MD. Hannington, and Shipboard Scientific Party; Report of *Somne* SO-133, BMBF FK 03G0133A, Freiberg University of Mining and Technology, p. 8–26.

Köster, H.M.
1960: Nontronite und picotit aus dem basalt des Okberges bei Hundsangen, Westerwald: Beitraege zur Mineralogie und Petrographie, v. 7, p. 71–77 (in German).

Murnane, R. and Clague, D.A.
1983: Nontronite from a low-temperature hydrothermal system on the Juan de Fuca Ridge; Earth and Planetary Science Letters, v. 65, p. 343–352.

Obina, B.
2000: A petrographic and chemical study of clay and associated minerals within indurated sediments (74 GTVA and 83 GTVA) retrieved from the Lihir Area, Papua New Guinea; B.Sc. thesis, Department of Earth Sciences, Carleton University, Ottawa, Ontario, 51 p.

Percival, J.B.
1994: Shipboard analyses; *in* Tectonics, Petrology and Hydrothermal Processes in Areas of Alkaline Island-Arc Volcanoes in the Southwest Pacific: The Tabar–Lihir–Tanga–Feni Island Chain, Papua New Guinea, (ed.) P.M. Herzig, MD. Hannington and Shipboard Scientific Party; Report of *Somne* SO-94, BMFT FK 03G0094A0, Freiberg University of Mining and Technology, p. 207–228.
1998: Shipboard analyses; *in* Volcanism, Hydrothermal Processes and Biological Communities at Shallow Submarine Volcanoes of the New Ireland Fore-Arc (Papua New Guinea), (ed.) P.M. Herzig, MD. Hannington, and Shipboard Scientific Party; Report of *Somne* SO-133, BMBF FK 03G0133A, Freiberg University of Mining and Technology, p. 118–130.

Percival, J.B., Ames, D.E.
1993: Clay mineralogy of active hydrothermal chimneys and an associated mound, Middle Valley, northern Juan de Fuca Ridge; Canadian Mineralogist, v. 31, p. 957–971.

Percival, J. B., Hannington, MD., Herzig, P.M., and Jonasson, I.R.
1999: Clay mineral associations in sulphide-bearing volcanic rocks and sediments from Lihir area, Papua New Guinea; *in* Proceedings of the 11th International Clay Conference, (ed.) H. Kodama, A.R. Mermut, and J.K. Torrance; Ottawa, Ontario, p. 689–696.

Weaver, C.E. and Pollard, L.D.
1973: The chemistry of clay minerals; Elsevier Scientific Publishing Company, Amsterdam, 213 p.

Velde, B.
1985: Clay minerals: a physico-chemical explanation of their occurrence; Elsevier Science Publishing Company Inc., Amsterdam, 427 p.

Winn, K., Horz, K., and Stoffers, P.
1998: Sedimentology; *in* Volcanism, Hydrothermal Processes and Biological Communities at Shallow Submarine Volcanoes of the New Ireland Fore-Arc (Papua New Guinea), (ed.) P.M. Herzig, MD. Hannington, and Shipboard Scientific Party; Report of *Somne* SO-133, BMBF FK 03G0133A, Freiberg University of Mining, p. 83–101.

Geological Survey of Canada Project 680023